MULTI-SYMBOL NONCOHERENT DETECTION OF MULTI-H CPM

Erik Perrins
Department of Electrical and Computer Engineering
Brigham Young University
Provo, UT 84602
esp@ee.byu.edu

Faculty Advisor:
Michael Rice

ABSTRACT

Two receivers are presented for the general case of noncoherent detection of multi-h continuous phase modulation (CPM). Both receivers yield performance gains using multi-symbol observations. The first is an existing receiver [1, 2] which has previously been applied to PCM/FM [3] and is now applied to the ARTM Tier II telemetry waveform. The second receiver is presented for the first time in this paper. The existing noncoherent receiver is found to perform poorly (and with high complexity) for the ARTM Tier II case. For single-symbol observations, the new receiver outperforms conventional FM demodulation for both telemetry waveforms, and for multi-symbol observation lengths its performance approaches that of the optimal coherent receiver. The performance is evaluated using computer simulations. Receiver performance is also evaluated using a simple channel model with varying carrier phase. The traditional FM demodulator approach is found to outperform both receivers as channel conditions worsen.

INTRODUCTION

The Advanced Range Telemetry (ARTM) Tier II modulation format is multi-h CPM. Some of the attractive features of this modulation format are that it has constant envelope and narrow bandwidth [4]. However, the existing optimal MLSE receiver for CPM [2] can have high complexity, both in trellis size and coherent demodulation requirements.

In this paper, two new receivers for multi-h CPM are presented. Both receivers are noncoherent and allow for multi-symbol observation. The first receiver is an existing receiver and has successfully been

applied to PCM/FM by Geoghegan [3], where a 5 symbol observation length was found to be 2.5 dB superior to traditional FM demodulation. One difficulty with the receiver is that the branch metrics are solely a function of the data in the multi-symbol observation window; meaning that the influence of previous observations is not passed along in the form of a cumulative path metric. The performance improves as the multi-symbol observation length increases; however, the penalty for this is that trellis complexity increases exponentially with increasing observation length. For the ARTM Tier II case, the existing receiver is found to perform poorly for practical multi-symbol observation lengths.

The second receiver is derived from a similar standpoint as the first. The novel element of the receiver is that it allows for the controlled use of a cumulative metric, where the reliance on past observations is adjusted using a so-called "forget factor". By including a cumulative metric, the receiver is able to perform well while keeping the multi-symbol observation length to a minimum. This new receiver performs well for both PCM/FM and ARTM Tier II waveforms. For PCM/FM, a two-symbol observation length (2 trellis states) is a few tenths of a dB inferior to the optimal maximum likelihood sequence estimating receiver (MLSE) in [2], and is 3.5 dB superior to conventional FM demodulation. For the ARTM Tier II case, the same two symbol observation length (64 states) is 2 dB inferior to the MLSE receiver and 4 dB superior to FM demodulation.

In the following, the CPM signal is summarized. The existing noncoherent receiver is then described. The second receiver is presented in detail, and the performance of the two receivers is examined with computer simulations. The simulations investigate the receiver performance under ideal conditions, and under a simple channel model with varying carrier phase.

CPM SIGNAL MODEL

CPM refers to a general class of digitally modulated signals in which the phase is constrained to be continuous. The complex-baseband signal may be expressed as

$$s(t) = \exp\big(j\psi(t,\boldsymbol{\alpha})\big) \tag{1}$$

$$\psi(t,\boldsymbol{\alpha}) = 2\pi \sum_{i=-\infty}^{n} \alpha_i h_{(i)} q(t-iT), \qquad nT < t < (n+1)T \tag{2}$$

where T is the symbol duration, $h_{(i)}$ are the modulation indices, $\boldsymbol{\alpha} = \{\alpha_i\}$ are the information symbols in the M-ary alphabet $\{\pm 1, \pm 3, \cdots, \pm(M-1)\}$, and $q(t)$ is the phase pulse. The subscript notation on the modulation indices is defined as

$$h_{(i)} \equiv h_{(i \bmod N_h)} \tag{3}$$

where N_h is the number of modulation indices (for the special case of single-h CPM, $N_h = 1$). The phase pulse $q(t)$ is related to the frequency pulse $f(t)$ by the relationship

$$q(t) = \int_0^t f(\tau)\, d\tau. \tag{4}$$

The frequency pulse is time-limited to the interval $(0, LT)$ and is subject to the constraints

$$f(t) = f(LT-t), \qquad \int_0^{LT} f(\tau)\, d\tau = q(LT) = \frac{1}{2}. \tag{5}$$

In light of the constraints on $f(t)$ and $q(t)$, Equation (2) can be written as

$$\psi(t,\boldsymbol{\alpha}) = \theta(t,\boldsymbol{\alpha}_n) + \theta_{n-L} = 2\pi \sum_{i=n-L+1}^{n} \alpha_i h_{(i)} q(t-iT) + \pi \sum_{i=-\infty}^{n-L} \alpha_i h_{(i)} \bmod 2\pi. \tag{6}$$

The term $\theta(t,\boldsymbol{\alpha}_n)$ is a function of the L symbols being modulated by the phase pulse. For $h_{(i)} = 2k_{(i)}/p$ ($k_{(i)}$, p integers), the phase state θ_{n-L} takes on p distinct values $0, 2\pi/p, 2\cdot 2\pi/p, \ldots, (p-1)2\pi/p$. The total number of states is pM^{L-1}, with M branches at each state. Each branch is defined by the $L+1$-tuple $\sigma_n = (\theta_{n-L}, \alpha_{n-L+1}, \alpha_{n-L+2}, \ldots, \alpha_n)$. The ARTM Tier II modulation is $M = 4$, $h = \{4/16, 5/16\}$ ($N_h = 2$), 3RC (raised cosine frequency pulse of length $L = 3$).

DECISION RULE FOR EXISTING NONCOHERENT RECEIVER

The model for the received complex-baseband signal is

$$r(t) = s(t,\boldsymbol{\alpha})e^{j\phi(t)} + n(t) \tag{7}$$

where $n(t) = x(t) + jy(t)$ is complex-valued additive white Gaussian noise with zero-mean and single-sided power spectral density N_0. The phase shift $\phi(t)$ introduced by the channel is unknown in general.

There are many instances where this signal model is considered. In [1], the binary CPFSK case is considered and $\phi(t)$ is assumed to be uniformly distributed over the interval $[-\pi, \pi]$. It is also assumed to be slowly varying so that it is constant over a multi-symbol observation interval NT. The receiver correlates the received signal against all possible transmitted sequences of length NT and outputs the maximum likelihood decision on the middle bit in the observation.

In [2](ch. 10), the more general CPM case is considered and $\phi(t)$ is modeled as a slowly varying process with the Tikhonov distribution. The Tikhonov distribution is parameterized by β and has three important special cases: the fully coherent case where $\beta = \infty$, the noncoherent case where $\beta = 0$ and $\phi(t)$ reduces to a uniformly distributed value over $[-\pi, \pi]$, and the partially coherent case where $0 < \beta < \infty$. A practical receiver is then given for the noncoherent case ($\beta = 0$), which is a generalization of the CPFSK receiver in [1]. This more general receiver has the complex-valued decision variable

$$\lambda_{\tilde{\alpha}}(n) = \int_{(n-N_1)T}^{(n+N_2)T} r(\tau) e^{-j\theta(\tau,\tilde{\alpha})} e^{-j\tilde{\theta}_{k-L}}\, d\tau, \qquad nT < t < (n+1)T, \quad kT \le \tau \le (k+1)T \tag{8}$$

$$\begin{aligned} = \lambda_{\tilde{\alpha}}(n-1) &- e^{-j\tilde{\theta}_{n-1-L-N_1}} \int_{(n-1-N_1)T}^{(n-N_1)T} r(\tau) e^{-j\theta(\tau,\tilde{\alpha})}\, d\tau \\ &+ e^{-j\tilde{\theta}_{n-1-L+N_2}} \int_{(n-1+N_2)T}^{(n+N_2)T} r(\tau) e^{-j\theta(\tau,\tilde{\alpha})}\, d\tau \end{aligned} \tag{9}$$

$$\tilde{\theta}_{k-L} = \pi \sum_{l=-\infty}^{k-L} \tilde{\alpha}_l h_{(l)} \bmod 2\pi \tag{10}$$

where $\tilde{\boldsymbol{\alpha}}$ is a hypothesized data sequence and the observation interval is $N_1 + N_2 = N$ symbol times. The term $\tilde{\theta}_{k-L}$ accumulates the phase of the hypothesized symbols after they have been modulated by the

length-LT phase pulse in $e^{-j\theta(\tau,\tilde{\alpha})}$; it is necessary to match the phase of the individual length-T segments of the integral in Equation (8). Equation (9) shows that this metric can be computed recursively using the Viterbi algorithm with a trellis of M^{L+N-2} states. It is important to point out that the recursion does not maintain a cumulative path metric, but rather functions as a sliding window that sums N individual length-T correlations (each rotated by the proper phase). The receiver does not perform a traceback operation to determine the output symbol, but instead outputs the symbol $\tilde{\alpha}_n$ corresponding to the metric $\lambda_{\tilde{\alpha}}(n)$ with the largest magnitude (the symbol $\tilde{\alpha}_n$ is the N_1-th symbol in the length-N observation, which is not necessarily the middle symbol). Since $\phi(t)$ is assumed to be constant over the N-symbol observation interval, the magnitude of the metric $\lambda_{\tilde{\alpha}}(n)$ is statistically independent of the channel phase.

There are two difficulties with the receiver described by Equation (8). The first is that the number of states grows exponentially with the observation interval N. The second is that, depending on the particular CPM scheme, a large value for N may be required to achieve adequate performance [2](ch. 10).

DECISION RULE FOR MODIFIED NONCOHERENT RECEIVER

A receiver that addresses these difficulties is described by the recursive metric

$$\lambda_{\tilde{\alpha}}(n) = a\lambda_{\tilde{\alpha}}(n-1) + e^{-j\hat{\theta}^{(i)}_{n-L}} z_{\tilde{\alpha}}(n) \tag{11}$$

$$z_{\tilde{\alpha}}(n) = \int_{nT}^{(n+1)T} r(\tau) e^{-j\theta(\tau,\tilde{\alpha})}\, d\tau \tag{12}$$

$$\hat{\theta}^{(i)}_{n-L} = \pi \sum_{k=-\infty}^{n-L} \hat{\alpha}^{(i)}_k h_{(k)} \bmod 2\pi \tag{13}$$

where the forget factor a is in the range $0 \le a \le 1$. The term $\hat{\theta}^{(i)}_{n-L}$ represents the phase contribution of all the previous symbol decisions $\hat{\alpha}^{(i)}_k$ for the i-th state in the trellis. Each state in the trellis stores two values: a cumulative metric $\lambda_{\tilde{\alpha}}(n-1)$, and a cumulative phase $\hat{\theta}^{(i)}_{n-L}$. The receiver uses a traceback matrix of length DD to output the symbol $\hat{\alpha}^{(i)}_{n-DD}$ corresponding to the state whose metric has the largest magnitude. Here, the branch metric $\lambda_{\tilde{\alpha}}(n)$ is only a function of the L symbols being modulated by the phase pulse $q(t)$, thus the number of states is M^{L-1}. For the special case of $a = 1$ this branch metric reduces to

$$\lambda_{\tilde{\alpha}}(n) = \sum_{k=-\infty}^{n} a^{n-i} e^{-j\hat{\theta}^{(i)}_{k-L}} \int_{kT}^{(k+1)T} r(\tau) e^{-j\theta(\tau,\tilde{\alpha})}\, d\tau \tag{14}$$

$$= \int_{-\infty}^{(n+1)T} r(\tau) e^{-j\theta(\tau,\tilde{\alpha})} e^{-j\hat{\theta}^{(i)}_{k-L}}\, d\tau, \qquad kT \le \tau \le (k+1)T. \tag{15}$$

This identifies an important tradeoff. As a approaches unity, the branch metric in Equation (11) approaches the one in Equation (15). The metric in Equation (15) is a loose approximation to an infinitely long observation interval because it "remembers" previous observations through the use of a cumulative metric. The optimal MLSE receiver also uses a cumulative metric to recursively compute a correlation from $(\infty, (n+1)T)$. The only difference here is the noncoherent receiver cannot account for the phase

states θ_{n-L} (shown in Equation (6)) in the trellis since the magnitude of the metrics (rather than the real part for the MLSE case) is used to determine survivors. However, when the slowly varying channel phase $\phi(t)$ is taken into account, the branch metric in Equation (15) will trace a curved path in the complex plane as $\phi(t)$ changes. This will reduce the magnitude of the metric and increase the probability that the competing paths through the trellis will have metrics with a magnitude larger then the true path. As a approaches zero, the branch metrics "forget" the infinite past more quickly and allow $\phi(t)$ to change more rapidly with less impact on the magnitude of the branch metrics.

EXTENDING THE DECISION RULE FOR MULTI-SYMBOL OBSERVATIONS

The metric in Equation (11) can be extended to more closely approximate an infinitely long observation interval. The reason for the inherently loose approximation in Equation (11) is that the trellis only allows for M^{L-1} states, when the underlying CPM signal is described by pM^{L-1} states, where the p-fold increase is due to the phase states θ_{n-L}. The extended metric for an observation interval of length $N \geq 1$ is given by

$$\lambda_{\tilde{\alpha}}(n) = a\lambda_{\tilde{\alpha}}(n-1) + e^{-j\hat{\theta}^{(i)}_{n-L-N+1}} z_{\tilde{\alpha}}(n) \tag{16}$$

$$z_{\tilde{\alpha}}(n) = e^{-j\tilde{\theta}_{n-L}} \int_{nT}^{(n+1)T} r(\tau) e^{-j\theta(\tau,\tilde{\alpha})}\, d\tau \tag{17}$$

$$\tilde{\theta}_{n-L} = \pi \sum_{k=n-L-N+2}^{n-L} \tilde{\alpha}_k h_{(k)} \bmod 2\pi. \tag{18}$$

The important difference between Equations (11)–(13) and Equations (16)–(18) is that $N-1$ symbols have been removed from the cumulative state phase $\hat{\theta}^{(i)}_{n-L-N+1}$ to form $\tilde{\theta}_{n-L}$, which is associated with the branch metric. This means that as paths merge and survivors are determined, we keep more options open in the trellis. The number of states in this trellis is M^{L-N-2}.

PERFORMANCE

For convenience, we will refer to the receiver defined in Equations (8)–(10) as "Receiver-A" and the receiver defined in Equations (16)–(18) as "Receiver-B" (Equations (11)–(13) are a special case of Receiver-B for $N = 1$). Both receivers have the parameter N, which is the multi-symbol observation length. Receiver-B is also parameterized by the forget factor a.

The first CPM scheme considered is the PCM/FM waveform in [3], which is $M = 2$, $h = 7/10$, 2RC (this is actually an approximation, where 2RC is very close to the fourth order Bessel pre-modulation filter used by Geoghegan). The performance of this waveform is given to demonstrate that the more general Receiver-A is equivalent to the receiver in [1, 3] for the $M = 2$ (binary) case. Three of the curves in Figure 1a appear in Geoghegan's paper: the one for the FM demodulator (FMD), and the two Receiver-A curves for the observation lengths $N = 3$ and $N = 5$. Figure 1a also shows two curves for Receiver-B, where the observation lengths are $N = 1$ and $N = 2$, and $a = 0.9$ (this value of $a = 0.9$ was found to yield the best receiver performance). The performance of the optimal MLSE receiver [2] is also shown as

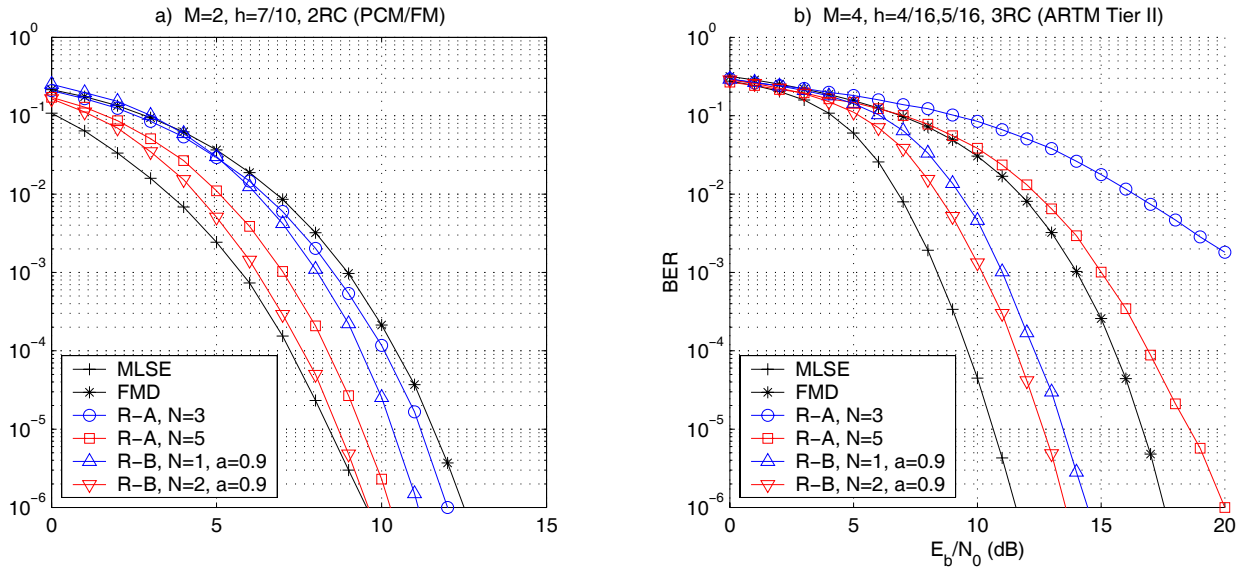

Figure 1: a) Six performance curves are shown for a PCM/FM waveform. Receiver-A is superior to the FMD for both observation lengths shown. Receiver-B is superior to Receiver-A, with appreciably less trellis complexity. Receiver-B performs close to the optimum receiver for $N = 2$. b) Six performance curves are shown for the ARTM Tier II waveform. Receiver-A performs poorly in this case, and is inferior to the FMD. Receiver-B demonstrates strong gains over the FMD, and is within 2 dB of the optimum receiver for $N = 2$.

a reference. As reported by Geoghegan, the Receiver-A with $N = 5$ yields an improvement of 2.5 dB over the traditional FMD. Figure 1a also shows that Receiver-B produces additional performance improvement over Receiver-A, in addition to requiring shorter observation intervals. At BER $= 10^{-6}$, Receiver-B with $N = 1$ performs with 1 dB improvement over Receiver-A with $N = 3$; these receivers have a trellis of 2 and 8 states respectively. A 0.7 dB improvement also exists for Receiver-B with $N = 2$ (4 states) over Receiver-A with $N = 5$ (32 states). Figure 1a indicates that Receiver-B with $N = 2$ performs very close to the optimal MLSE receiver, which shows there is little to be gained by further increasing N for this CPM scheme.

The next CPM scheme in the simulations is the ARTM Tier II waveform, which is $M = 4$, $h = \{4/16, 5/16\}$, 3RC. Figure 1a shows the same set of six curves in the previous PCM/FM example. Here the results are very different. Receiver-A is shown to perform at a loss relative to the FMD. At BER $= 10^{-6}$ this loss is 1 dB for $N = 5$, and 7 dB for $N = 3$. This is a surprising result when considering that these receivers have 4096 and 256 states respectively. The sharp difference in the performance of Receiver-A for these two CPM schemes would likely be explained by differences in distance properties of the two waveforms under noncoherent reception. In [2](ch. 10) it is shown that some CPM schemes require much larger values of N to achieve noncoherent performance close to the coherent case; However, analysis of this sort has not been performed for the ARTM Tier II case at this time. For the case of Receiver-B, it outperforms the FMD by several dB at BER $= 10^{-6}$, and is only 2 and 3 dB inferior to the optimum MLSE receiver for $N = 2$ and $N = 1$ respectively (64 and 16 states each).

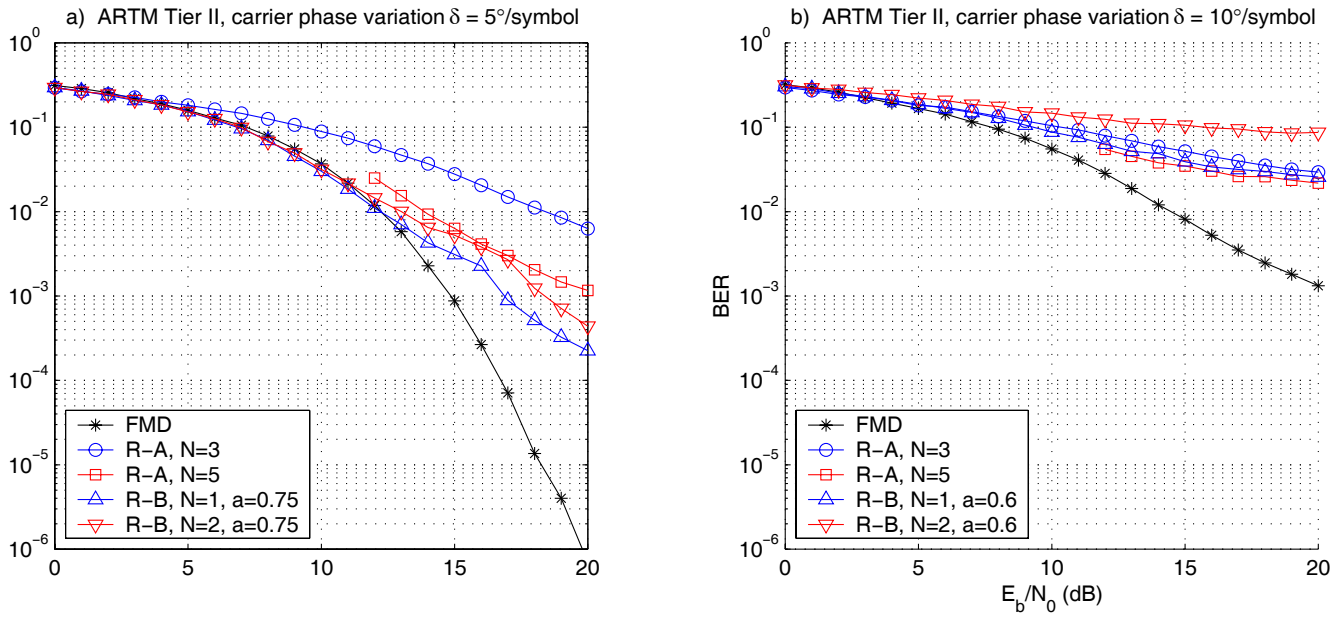

Figure 2: a) Performance curves are shown for the channel where $\delta = 5°/\text{symbol}$. The FMD outperforms both Receivers-A and -B. For Receiver-B, the less complex case where $N = 1$ is superior to the more complex $N = 2$. b) Performance curves are shown for $\delta = 5°/\text{symbol}$. For both channel cases, the forget factor a was reduced to achieve better performance.

Up to this point, we have only considered performance for the case of perfect symbol timing and carrier phase. Since the motivation for a noncoherent receiver is the case where the carrier phase is not known and assumed to be varying, a simple model will be introduced for variations in the carrier phase. Let [5]

$$\phi_n \equiv \phi(nT) = \phi_{n-1} + \nu_n \bmod 2\pi \tag{19}$$

where $\{\nu_n\}$ are independent and identically distributed Gaussian random variables with zero mean and variance δ^2. This models the phase noise as a first order Markov process with Gaussian transition probability distribution. For perfect carrier phase tracking, $\delta = 0$.

Figure 2a shows the performance the ARTM Tier II waveform with the two receivers for the case where $\delta = 5°/\text{symbol}$. Among the noncoherent receivers, the traditional FMD performs best for this particular channel model. What is particularly interesting is that in the case of Receiver-B, the shorter observation interval ($N = 1$) outperforms the longer one ($N = 2$). Also, a lower value of $a = 0.75$ was found to yield the best performance under these channel conditions. These performance characteristics of Receiver-B would appear to be a result of the very structure of the receiver. Under these channel conditions, lowering the value of the forget factor reduces the dependence of the branch metrics on previous noisy observations. Increasing the observation length under these channel conditions would only exacerbate the situation by increasing the reliance on previous noisy observations. Figure 2b shows that when δ is increased to $10°/\text{symbol}$ the performance of Receiver-B with $N = 2$ is the worst (note that a was further reduced to 0.6). For both values of δ, Receiver-B with $N = 1$ (2 states) outperformed Receiver-A with $N = 5$ (4096 states), and the FMD outperformed them all.

DISCUSSION AND CONCLUSIONS

Geoghegan has found Receiver-A to be an attractive alternative to the conventional FMD receiver design for the case of PCM/FM [3]. The performance results presented here show that this is not the case for the ARTM Tier II waveform. The case for Receiver-A is further eroded by its high complexity.

A new design for a noncoherent receiver was presented (Receiver-B) which allows for multi-symbol observations and an adjustable dependence on previous observations. The controlled use of a cumulative metric by this receiver is an important difference from Receiver-A. This receiver was found to perform well with low complexity (single-symbol observations) for both CPM schemes (PCM/FM and ARTM Tier II).

An additional dimension of receiver performance was modeled by simulating a channel with random phase variations. In this case, the traditional FMD outperformed both Receivers-A and -B. It was also found that Receiver-B performed best under these channel conditions when its reliance on previous observations was reduced (i.e. lowering the forget factor a) and using single-symbol observations.

Future work might be done to analytically explain some of the simulation results; including the exact cause of Receiver-A's poor performance with the ARTM Tier II waveform, and the reasons for Receiver-B's behavior under harsh channel conditions. Also, work could be done to derive an analytical expression for the performance of Receiver-B. This would shed light on optimal values for the receiver parameters N and a. Work might also be done to investigate an adaptive means of adjusting the forget factor of Receiver-B as channel conditions change.

REFERENCES

[1] W. P. Osborne and M. B. Luntz. "Coherent and noncoherent detection of CPFSK". *IEEE Transactions on Communications*, 22(8):1023–1036, August 1974.

[2] J. B. Anderson, T. Aulin, C-E. Sundberg. *Digital Phase Modulation*. Plenum Press, New York, 1986.

[3] M. Geoghegan. "Improving the detection efficency of conventional PCM/FM telemetry by using a multi-symbol demodulator". In *Proceedings of the International Telemetering Conference*, San Diego, CA, October 2000.

[4] M. Geoghegan. "Description and performance results for the advanced range telemetry (ARTM) Tier II waveform". In *Proceedings of the International Telemetering Conference*, San Diego, CA, October 2000.

[5] D. Raphaeli and D. Divsalar. "Noncoherent detection of continuous phase modulation using overlapped observations". In *Proceedings of the Global Telecommunications Conference (GLOBECOMM)*, pages 191–195, November 1994.